Cell Transplantation, Vol. 26, pp. 753–764, 2017

0963-6897/17 $90.00 + .00
DOI: https://doi.org/10.3727/096368917X695029
E-ISSN 1555-3892
www.cognizantcommunication.com

Hydrogen Sulfide Reduces Recruitment of CD11b$^+$Gr-1$^+$ Cells in Mice With Myocardial Infarction

Ting Wu,*[1] Hua Li,†‡[1] Bing Wu,* Lei Zhang,* San-wu Wu,* Jia-ning Wang,* and You-en Zhang*

*Department of Cardiology, Renmin Hospital, Hubei University of Medicine, Shiyan, P.R. China
†Shanghai Institute of Cardiovascular Diseases, Zhongshan Hospital, Fudan University, Shanghai, P.R. China
‡State Key Laboratory of Cell Biology, Institute of Biochemistry and Cell Biology, Shanghai, P.R. China

The present study aimed to elucidate the mechanisms by which hydrogen sulfide (H_2S) attenuates left ventricular remodeling after myocardial infarction (MI). MI was created in mice by left coronary artery ligation. One group of mice received injections of the H_2S donor sodium hydrosulfide (NaHS) immediately before and 1 h after ligation, while the control group received saline alone. During both the subacute and chronic stages (1 and 4 weeks postinfarction, respectively), NaHS-treated mice demonstrated attenuation of cardiac dilation in the infarcted myocardium. Furthermore, fewer CD11b$^+$Gr-1$^+$ myeloid cells were detected in the infarct myocardium and peripheral blood from NaHS-treated mice, while more CD11b$^+$Gr-1$^+$ cells remained in the spleen and bone marrow in these animals. NaHS-treated mice also exhibited reduction in cardiomyocyte apoptosis, interstitial fibrosis, cardiac hypertrophy, and pulmonary edema, as well as overall better survival rates, when compared to controls. Thus, exogenous H_2S has favorable effects on cardiac remodeling after MI. These observations further support the emerging concept that H_2S treatment might have therapeutic benefits in the setting of ischemia-induced heart failure.

Key words: Hydrogen sulfide (H_2S); Inflammation; Myeloid cells; Cardiac remodeling; Myocardial infarction (MI)

INTRODUCTION

Despite the fact that many novel therapeutic approaches for patients with chronic heart failure have been evaluated in clinical trials, the risk of heart failure following myocardial infarction (MI) has remained high, and effective therapies continue to be elusive[1]. Several studies of clinical and experimental MI have suggested a new possibility, however, by providing compelling evidence that inflammatory signals recruit neutrophils to the infarct zone within 24 h and monocytes/macrophages shortly thereafter[2,3]. Therefore, understanding the role of inflammatory response in myocardial insult and postischemic scar formation may guide future therapeutic strategies.

Hydrogen sulfide (H_2S), first described as a physiological mediator in the brain in 1996 and in the cardiovascular system the following year[4], has drawn considerable attention for its role in various (patho)physiological processes. It is acknowledged as the third gasotransmitter, after nitric oxide (NO) and carbon monoxide (CO), and shares many functions with those gases. H_2S biosynthesis has been identified in a variety of mammalian tissues, notably in the brain, heart, and gastrointestinal tract, as well as in isolated vascular smooth muscle and endothelial cells and neurons[5]. Three H_2S-generating enzymes have been characterized in mammals: cystathionine β-synthase (CBS), cystathionine γ-lyase (CSE), and 3-mercaptopyruvate sulfurtransferase (3MST). There is growing evidence that H_2S-producing enzymes and H_2S plasma levels are reduced in various diseases[6–8]. In addition, the role of this gaseous mediator in cardiovascular homeostasis[9–11] and in various conditions associated with both pro- and anti-inflammatory signaling[12,13] has been elucidated.

We found previously that the exogenous H_2S donor sodium hydrosulfide (NaHS) has potent anti-inflammatory effects in hearts subjected to acute MI in vivo and that this may be due in part to decreased recruitment of CD11b$^+$ Gr-1$^+$ myeloid cells[14], which, as a regulatory component of

Received August 24, 2016; final acceptance March 2, 2017. Online prepub date: February 9, 2017.
[1]These authors provided equal contribution to this work.
Address correspondence to You-en Zhang, Ph.D., Institute of Clinical Medicine and Department of Cardiology, Renmin Hospital, Hubei University of Medicine, No. 39 Chaoyang Road, Shiyan 442000, P.R. China. Tel: +86-0719-8637305; E-mail: zye112@hotmail.com

the innate immune response, are presumed to play an important role in the inflammatory process after MI. In addition, we have shown that NaHS prevents transforming growth factor-β1 (TGF-β1)-induced fibroblast-to-myofibroblast transformation, as well as proliferation, migration, and collagen synthesis[15]. In this study, we investigated the effect of NaHS on subacute and chronic heart failure (1 and 4 weeks postinfarction, respectively) in a mouse model. The results show that NaHS decreases the severity of all outcomes measured, including recruitment of $CD11b^{+}Gr\text{-}1^{+}$ myeloid cells to the peripheral circulation, suggesting that NaHS-induced reduction of heart failure following MI may be due in part to the effect of H_2S on the innate immune system.

MATERIALS AND METHODS

Animals and Induction of Heart Failure

C57BL/6J mice (20–25 g, male, 8–10 weeks; Slac Laboratory, Shanghai, P.R. China) were housed under standard conditions in a temperature-controlled room with a 12:12-h light/dark cycle. Their diet consisted of normal mouse chow and water ad libitum. This study was carried out in strict accordance with the recommendations in the guide for the Animal Management Rules of the Ministry of Health of the People's Republic of China. The protocol was approved by the Committee on the Ethics of Animal Experiments of Fudan University. All surgery was performed under anesthesia, and all efforts were made to minimize suffering.

Heart failure was induced by permanent ligation of left coronary artery ligation as described previously[14]. Briefly, mice were anesthetized with 2% isoflurane inhalation and then intubated with a 22-gauge intravenous catheter and ventilated with a mixture of O_2 and 1%–2% isoflurane. A left thoracotomy was performed through the fourth intercostal space transversely to expose the thoracic cage. After the pericardium was opened, the left coronary artery was identified and occluded by an 8-0 silk ligature. Successful ligation was confirmed when the anterior wall of the left ventricle (LV) turned pale. Sham-operated animals underwent the same procedure without ligation of the coronary artery. Autopsies were performed on any mice that died during surgery to determine the cause of death. Cardiac rupture was confirmed by the presence of blood coagulation around the pericardial sac and in the chest cavity, and heart failure was diagnosed by lung congestion with chest fluid accumulation.

H_2S Treatment

H_2S was administered in the form of NaHS, which was obtained from Sigma-Aldrich (St. Louis, MO, USA). NaHS was diluted in normal (0.9%) saline to the desired concentration immediately before administration by intraperitoneal (IP) injection. Saline was administered in the same manner in the control groups.

Experimental Groups

Four groups were used: (1) sham + saline ($n = 12$): each mouse received 100 µl of normal (0.9%) saline (IP) 5 min before and 60 min after sham surgery; (2) sham + NaHS ($n = 12$): each mouse received 1 mg/kg NaHS in 100 µl of normal (0.9%) saline (IP) 5 min before and 60 min after sham surgery; (3) MI + saline ($n = 46$): each mouse received 100 µl of normal (0.9%) saline 5 min before and 60 min after coronary artery occlusion; and (4) MI + NaHS ($n = 46$): each mouse received 1 mg/kg NaHS in 100 µl of normal (0.9%) saline (IP) 5 min before and 60 min after coronary artery occlusion.

Survival

Survival rate was calculated for each experimental group as: number of mice surviving at a given time/number of mice that recovered from surgery.

Evaluation of Cardiac Hypertrophy and Pulmonary Edema

Cardiac hypertrophy and pulmonary edema were evaluated at week 4 after surgery for five surviving mice from each group. Mice were weighed and then sacrificed. The hearts and lungs were collected and weighed immediately after collection. Cardiac hypertrophy was calculated as the ratio of heart weight (mg) to body weight (g). Pulmonary edema was calculated as the ratio of lung weight (mg) to body weight (g).

Echocardiography

In vivo cardiac geometry and function were serially assessed by transthoracic echocardiography performed with a Vevo 770 imaging system (VisualSonics, Inc., Toronto, Canada) on weeks 1 and 4 after surgery before the animals were euthanized. Eight to 10 mice from each group were evaluated. Mice were sedated with 1%–2% isoflurane and placed on a heating pad to maintain body temperature. A short-axis view of the LV at the level of papillary muscle was obtained, and at least three consecutive beats were evaluated. LV wall thickness and internal dimensions were measured, and the LV ejection fraction (LVEF) was calculated.

^{18}F-FDG Positron Emission Tomography/Computed Tomography (PET/CT) Scanning

PET/CT scanning was performed 1 week after surgery on four mice from each group. Mice were fasted for 12 h but had unrestricted access to water. Following determination of body weights (24.0 ± 5.10 g on average), mice were anesthetized with ketamine (100 mg/kg). Sterile

normal saline (0.1 ml) was injected subcutaneously to ensure adequate hydration. Following administration of ^{18}F-fluorodeoxyglucose [FDG; 15 megabecquerel (MBq) in 100 μl; Siemens Healthcare, Erlangen, Germany] via lateral tail vein injection, mice were awakened and returned to individual holding cages. Precisely 60 min after ^{18}F-FDG injection, mice were reanesthetized using isoflurane (4% for induction, 1%–2% for maintenance) and were placed on a heating pad to maintain body temperature during data acquisition. The midmyocardial contours for myocardial regions with normal ^{18}F-FDG uptake and, in the case of the postinfarction scans, for regions with markedly reduced ^{18}F-FDG uptake implying nonviability were interactively traced. The uptake of myocardial ^{18}F-FDG [3D regions of interest (ROI)] was analyzed with the Inveon Research Workplace 3.0 software (Siemens Healthcare, Deerfield, IL, USA). The results were expressed as the mean standardized uptake value (SUV).

Evaluation of Apoptosis

To detect apoptosis, LV tissue sections were labeled with terminal deoxynucleotidyl transferase-mediated 2′-deoxyuridine 5′-triphosphate (dUTP) nick-end labeling (TUNEL; ApopTag HRP kit; DBA Italia S.r.l., Milan, Italy). The apoptosis rate was expressed as the number of TUNEL-positive nuclei out of the total nuclei per field and was calculated in five random fields for each section. The pathologist who scored the TUNEL results was blinded to the treatment.

Histopathology

Heart tissue collected from four to six mice per group at 4 weeks after surgery was fixed in formalin, embedded in paraffin, and cross-sectioned at 4 μm from base to apex. Sections were stained with hematoxylin and eosin (H&E; Nanjing Jiancheng Biological Engineering Institute, Nanjing, P.R. China) and with Masson trichrome (Nanjing Jiancheng Biological Engineering Institute), which stains collagen blue. Collagen deposition was used as an indication of cardiac fibrosis. Three representative sections of each heart were examined and scored in a blinded manner using ImagePro software (Media Cybernetics, Inc., Rockville, MD, USA). Collagen content was calculated as percentage of blue-stained area in relation to the total heart tissue area.

Transmission Electron Microscopy (TEM)

Myocardium harvested 4 weeks after surgery was fixed with 2.5% glutaraldehyde (Sigma-Aldrich), then fixed with 1% osmium tetroxide (Sigma-Aldrich) and dehydrated in a conventional ethanol gradient. After epoxy resin embedding and deployment of a hardener, accelerator, and growth agent, ultrathin sections with a thickness of 50 nm were cut by ultramicrotomy and stained with uranyl acetate and lead citrate (Sigma-Aldrich) solution. Changes in the myocardial ultrastructure were observed with a JEM-1200EX TEM (JEOL Ltd., Tokyo, Japan). The required area was selected for image capture.

Flow Cytometry for Detection of $CD11b^+Gr\text{-}1^+$ Myeloid Cells

On 1 and 4 weeks after MI, peripheral blood, splenocytes, bone marrow-derived cells from the femur, and heart were isolated and processed as previously described[14,16]. In brief, whole blood, spleen, bone marrow, and heart were drawn and subjected to red cell lysis (BD Biosciences, Franklin Lakes, NJ, USA). Single-cell suspensions were made by filtering through a 40-μm strainer mesh, and cells were labeled with fluorochrome-conjugated mouse-specific antibodies against CD11b and Gr-1 (BD Biosciences) and were evaluated by multicolor flow cytometry using an LSR II flow cytometer (BD Biosciences). Data were analyzed using FlowJo 7 software (Tree Star, Inc., Ashland, OR, USA).

Measurement of Cytokines

Blood was collected by cardiac puncture at the time of sacrifice. The samples were centrifuged, and the serum was collected. The expression of tumor necrosis factor-α (TNF-α) and interleukin-1β (IL-1β) cytokines were measured using an ELISA Kit (R&D Systems, Minneapolis, MN, USA).

Statistical Analysis

Data are expressed as mean±standard error of the mean (SEM) unless otherwise indicated. Differences between the groups were compared with one-way analysis of variance (ANOVA) where appropriate with post hoc Tukey test or Bonferroni analysis. Survival rates were compared by the Kaplan–Meier method and analyzed by the log-rank test. Values of $p<0.05$ were considered statistically significant. Statistical analysis was performed with Statistical Package for the Social Sciences (SPSS) Statistics 17.0 program (IBM Corporation, Armonk, NY, USA).

RESULTS

NaHS Improves Survival After Permanent Coronary Occlusion

Survival rates for the four experimental groups (sham+saline, sham+NaHS, MI+saline, and MI+NaHS) were determined at various times throughout the 4 weeks following surgery (Fig. 1). The survival curves were statistically different ($p<0.05$) by log-rank test. At 28 days, the final time point, 23 of 46 (50%) mice in the MI+NaHS group survived, a significantly higher survival rate than the 15 of 46 (33%; $p<0.05$) in the MI+saline group.

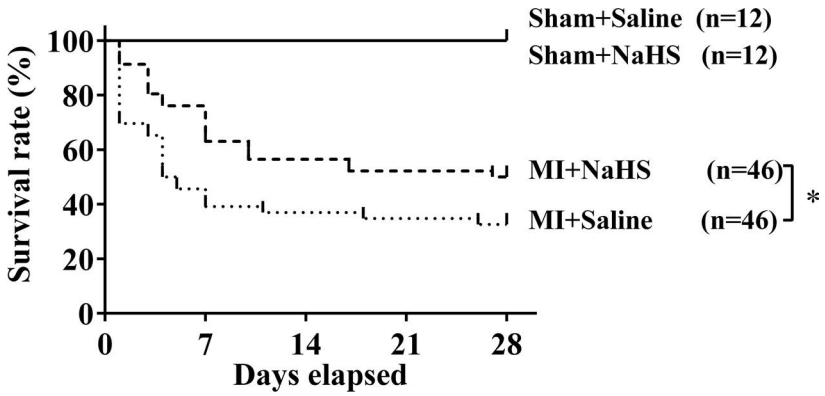

Figure 1. Kaplan–Meier survival analysis. Percentages of surviving mice after sham operation or coronary occlusion were plotted. The survival curves were statistically different (*$p<0.05$) by log-rank test. NaHS, sodium hydrosulfide; MI, myocardial infarction.

All sham-operated mice survived throughout the study. These findings suggest that NaHS treatment protects mice from heart failure following coronary artery occlusion.

NaHS Attenuates Cardiac Hypertrophy and Pulmonary Edema Following Coronary Occlusion

Four weeks after coronary occlusion, both mean heart weight-to-body weight ratio (a measure of cardiac hypertrophy) and mean lung weight-to-body weight ratio (a measure of pulmonary edema) were significantly lower in the NaHS-treated group than that in the saline control group ($p<0.05$) (Fig. 2). Thus, NaHS treatment may also protect from development of cardiac hypertrophy and pulmonary edema in mice after coronary artery occlusion.

NaHS Mitigates Cardiac Dilation and Improves Cardiac Ejection Fraction After Coronary Artery Occlusion

At 1 week and 4 weeks after surgery, a subset of surviving mice were subjected to echocardiography evaluation to determine the degree of left ventricular (LV) hypertrophy, dilatation, and resulting dysfunction (Fig. 3A). Analysis showed that, at both time points, mice in the MI+NaHS group had significantly lower LV end-diastolic dimension (LVEDD; $p<0.05$) (Fig. 3B) and LV end-systolic dimension

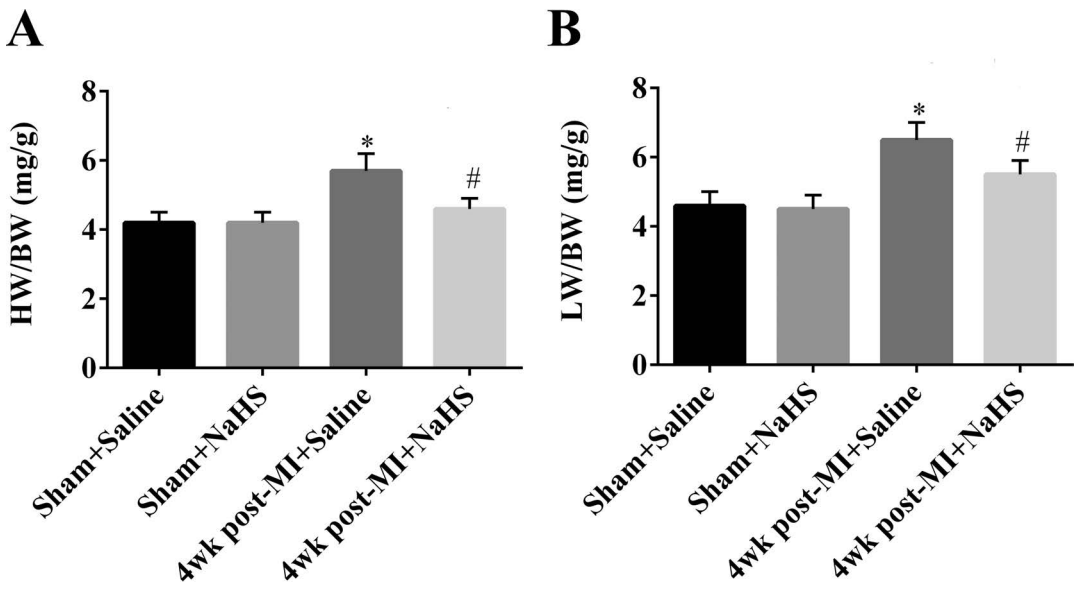

Figure 2. Cardiac hypertrophy and pulmonary edema 4 weeks after coronary occlusion or sham surgery. The ratio of heart weight (HW; in mg) to body weight (BW; in g) was determined in the four experimental groups ($n=5$ per group) as a measure of cardiac hypertrophy (A). The ratio of lung weight (LW; in mg) to BW (in g) was determined in the four experimental groups ($n=5$ per group) as a measure of pulmonary edema (B). *$p<0.05$, MI+saline versus sham+saline; #$p<0.05$, MI+NaHS versus sham+NaHS. NaHS, sodium hydrosulfide; MI, myocardial infarction; NS, not significant; wk, week.

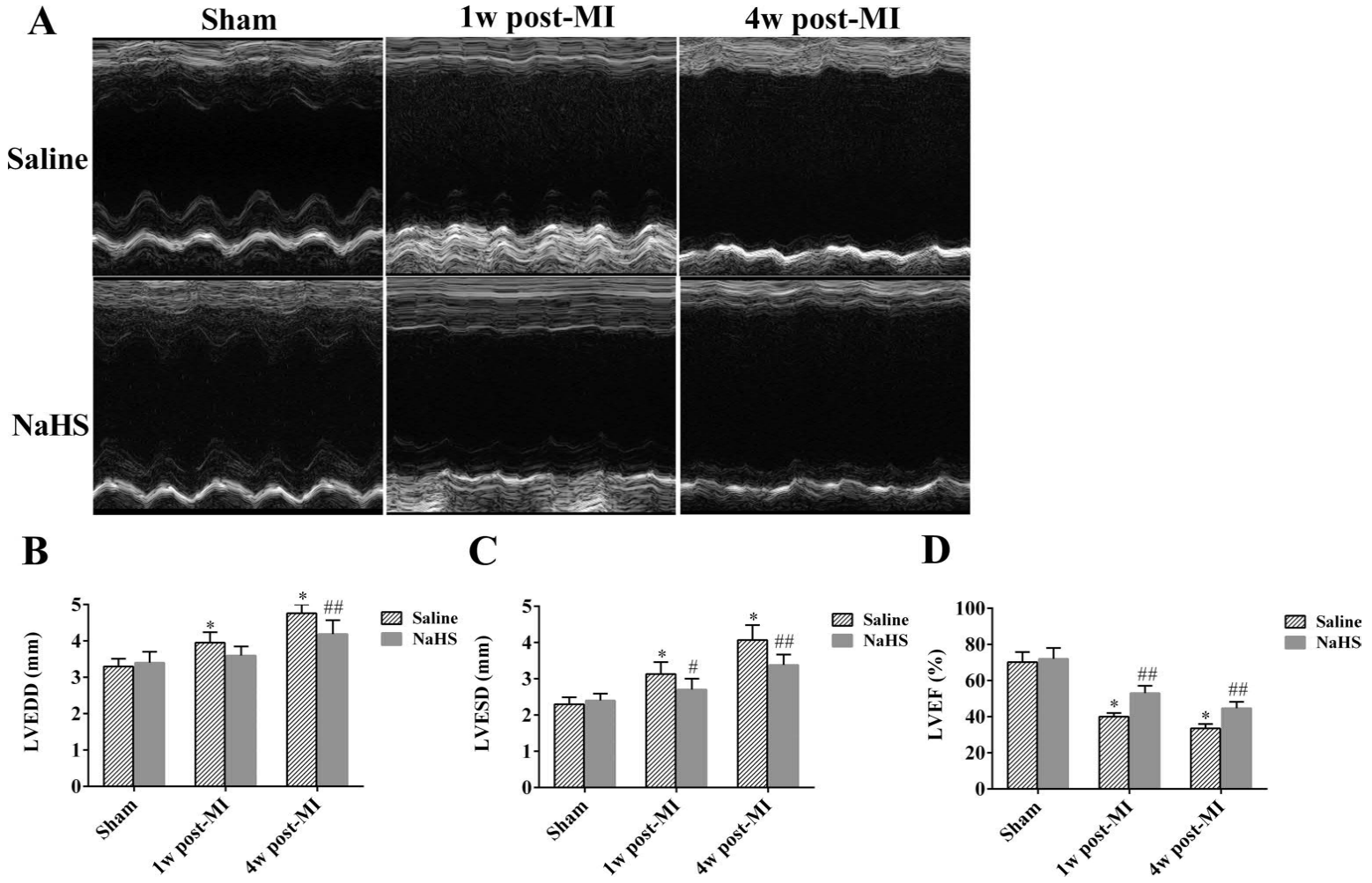

Figure 3. Echocardiographic parameters of mice with ischemia-induced heart failure. Representative M-mode measurement (A) and echocardiographic results of left ventricular end-diastolic diameter (LVEDD) (B), end-systolic diameter (LVESD) (C), and ejection fraction (LVEF) (D) in the various treatment groups. Measurements made 1 week after surgery for sham groups and 1 week and 4 weeks after surgery for the MI groups. $n = 8–10$ for all treatment groups. *$p < 0.01$, MI + saline versus sham + saline; #$p < 0.05$, ##$p < 0.01$, MI + NaHS versus sham + NaHS. NaHS, sodium hydrosulfide; MI, myocardial infarction; NS, not significant; w, week.

(LVESD; $p<0.05$) (Fig. 3C), and significantly higher LV ejection fraction (LVEF; $p<0.05$) (Fig. 3D), compared to the MI+saline group. Thus, exogenous NaHS treatment can have profound reciprocal effects on ischemia-induced heart failure, in terms of both LV structure and cardiac function, in both the subacute and chronic phases.

NaHS Prevents Myocardial Infarct Expansion and Reduces Apoptosis Following Coronary Occlusion

PET/CT images showed that the ^{18}F-FDG signal within myocardial infarcts 1 week after surgery was significantly lower in the MI+saline group compared to the sham group ($p<0.05$). In the MI+NaHS group, the ^{18}F-FDG signal

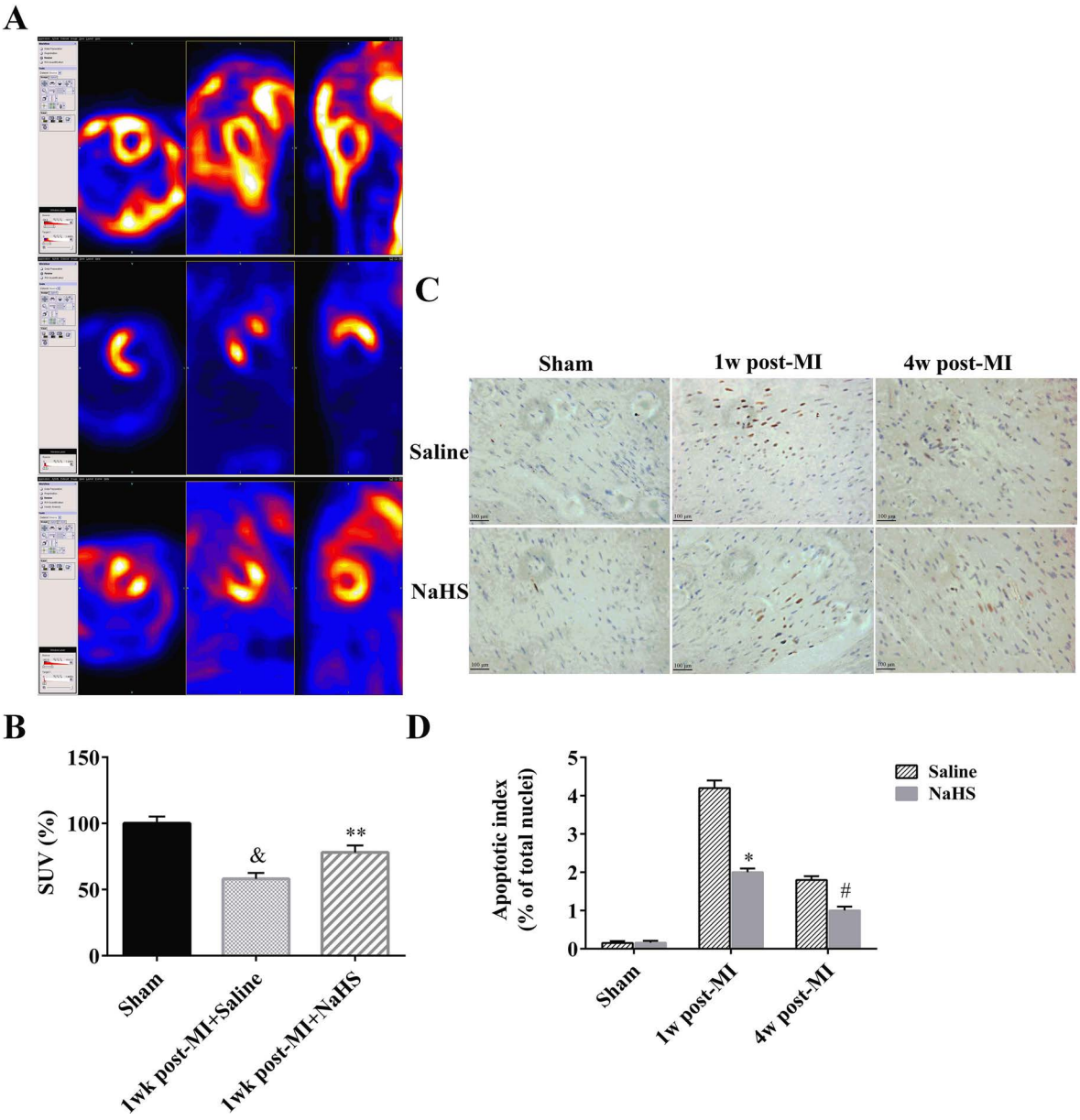

Figure 4. Cardioprotective effects of NaHS as measured by PET/CT and TUNEL apoptosis assay. PET/CT was performed 1 week after surgery. Representative PET/CT images of coronal whole-body slice at the level of left ventricle are shown. Left: horizontal view of the heart; middle: side view of the heart; right: front view of the heart (A). PET/CT standard uptake values (SUV) determined by manual delineation ($n=4$) (B). Representative TUNEL assay images (200×) (C). Quantification of TUNEL-positive cells (percentage of total nuclei; $n=5$ hearts per group) (D). Scale bars: 100 μm. &$p<0.05$, 1 week post-MI+saline versus sham. *$p<0.05$, MI+saline versus sham+saline; **$p<0.01$, MI+saline versus sham+saline; #$p<0.01$, MI+NaHS versus sham+NaHS. NaHS, sodium hydrosulfide; MI, myocardial infarction; NS, not significant; PET/CT, positron emission tomography–computed tomography; TUNEL, terminal deoxynucleotidyl transferase 2′-deoxyuridine 5′-triphosphate (dUTP) nick–end labeling; w, week.

was somewhat lower than in the sham group, although not significantly lower, but was significantly higher than in the MI + saline group ($p < 0.05$) (Fig. 4A and B), suggesting that administration of NaHS leads to decreased infarct size in the subacute phase. To confirm this cardioprotective effect in the subacute phase and investigate effects in the chronic phase, apoptosis in cardiac samples taken 1 and 4 weeks after surgery was quantified using the TUNEL assay. At both time points, the number of apoptotic cells was significantly increased in both MI groups compared to the Sham + saline control group. However, the number of apoptotic cells was significantly lower in the MI + NaHS group compared to the MI + saline group at both time points ($p < 0.05$) (Fig. 4C and D), confirming the cardioprotective effect of NaHS.

NaHS Decreases Collagen Accumulation Following Coronary Occlusion in Mice

Masson trichrome staining and TEM were used to evaluate collagen deposition and fibrosis in heart tissue 4 weeks after surgery. Tissue from MI + NaHS mice showed less collagen deposition than that from MI + saline mice ($p < 0.05$), suggesting that NaHS treatment limits interstitial fibrosis in the infarct areas (Fig. 5A–C). NaHS had no effect on collagen deposition in the sham animals. These observations were confirmed by TEM, which showed that the number of collagen fibers was increased in the connective tissue of hearts from mice in the MI groups compared to sham, and similar to the results with Masson trichrome staining, NaHS treatment reduced the number of collagen fibers in MI mice (Fig. 5D).

NaHS Affects Recruitment and Migration of $CD11b^+Gr\text{-}1^+$ Myeloid Cells

One important cardioprotective property of NaHS is its inhibitory effect on inflammatory cell trafficking[10]. To determine the specific effect of NaHS on $CD11b^+Gr\text{-}1^+$ myeloid cells during the subacute and chronic stages of infarction, flow cytometry was used to quantify $CD11b^+Gr\text{-}1^+$ cells in the myocardium, peripheral blood, spleen, and bone marrow collected from MI + saline and MI + NaHS at 1 week and 4 weeks after coronary occlusion, and from sham + saline and sham + NaHS at 4 weeks after surgery. At 1 week, $CD11b^+Gr\text{-}1^+$ cell number was significantly increased in the myocardium from MI + saline mice. $CD11b^+Gr\text{-}1^+$ cell number was also increased in the myocardium from MI + NaHS mice but was significantly lower than in the myocardium from MI + saline mice ($p < 0.05$) (Fig. 6A and B). By 4 weeks after occlusion, $CD11b^+Gr\text{-}1^+$ cell number had returned to normal in the myocardium from both MI groups. Similar results were observed in peripheral blood (Fig. 6C and D). $CD11b^+Gr\text{-}1^+$ myeloid cell number was further evaluated in the spleen and bone marrow. At 1 week after occlusion, $CD11b^+Gr\text{-}1^+$ cell number was significantly decreased in the spleen from both MI groups, compared to sham control, but the number in the MI + NaHS spleen was significantly higher than that in the MI + saline spleen. At 4 weeks after occlusion, $CD11b^+Gr\text{-}1^+$ cell number was back to normal in the MI + NaHS spleen but was still significantly lower in the MI + saline spleen (Fig. 6E and F). Similar results were seen in the bone marrow in the MI + saline group (Fig. 6G and H).

NaHS Decreases Systemic Inflammation Responses in the Subacute Phase of Infarction

To investigate the effects of NaHS on the inflammatory response, serum levels of TNF-α and IL-1β were measured at 1 and 4 weeks after coronary occlusion. ELISA analysis revealed significant increases in both TNF-α and IL-1β in the MI + saline and MI + NaHS groups 1 week after occlusion, compared with the sham group (Fig. 7A and B), but TNF-α and IL-1β levels were significantly lower in the MI + NaHS group compared to the MI + saline group. At 4 weeks after surgery, TNF-α and IL-1β levels were back to normal in both MI groups.

DISCUSSION

MI leads to an inflammatory response characterized by the generation of proinflammatory mediators and an influx of leukocytes that are necessary to remove necrotic cellular debris and promote recovery of LV contractile function. However, an improperly regulated inflammatory response and pathological LV remodeling could impair LV function and lead to heart failure and death after MI. LV remodeling after MI is the process of infarct expansion followed by noninfarct hypertrophy, which promotes heart failure under the condition of poor prognosis, such as defective infarct healing or excessive infarct size and wall stress. Ample evidence from experimental models of myocardial ischemia suggests that defects in pathways involved in timely suppression, resolution, and containment of the postinfarction inflammatory response result in adverse remodeling of the infarct heart[2,17,18]. Despite growing understanding of the chronic inflammatory nature of cardiac remodeling and the fact that strategies targeting mediators of inflammation such as lipoxygenase[19], complement[20], or cytokines[21] have demonstrated efficacy in experimental models, specific anti-inflammatory therapies for MI have not yet materialized.

In recent years, the cardioprotective effects of H_2S have been demonstrated in various models of myocardial injury. A single administration of H_2S before, during, or after myocardial ischemia has been shown to decrease myocardial infarct size and attenuate LV dysfunction in both rodents and pigs[22–24]. Based on these previous studies, the present study focused on the therapeutic role of H_2S in long-term protection against myocardial injury.

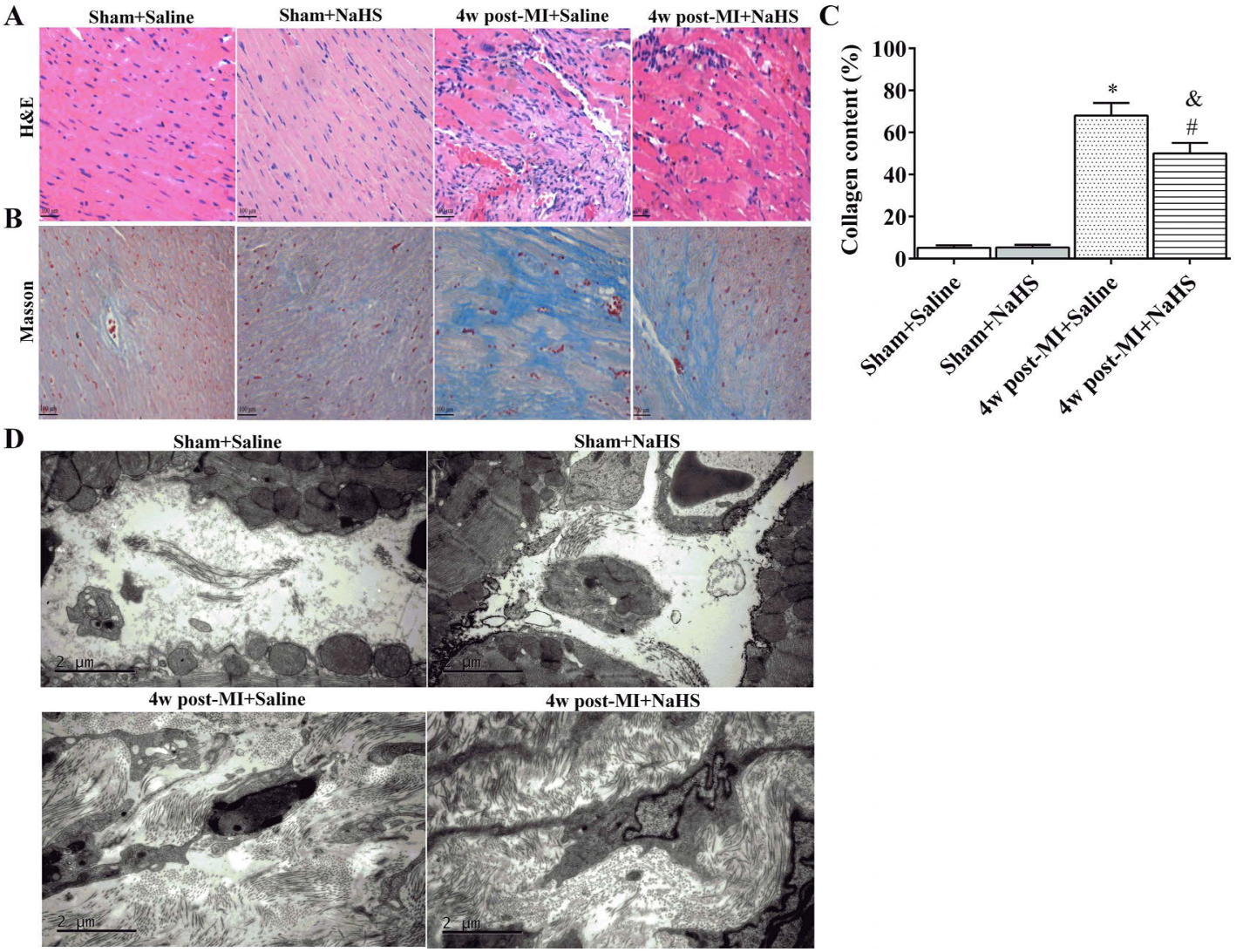

Figure 5. Collagen deposition and fibrosis in cardiac muscle 4 weeks after surgery. Transverse sections of hearts stained with H&E (A; 200×; scale bars: 100 μm) and Masson trichrome (blue staining indicates collagen) (B; 200×; scale bars: 100 μm). Relative area of collagen, as indicated by blue stain, was measured among various groups. Whole section area was set as 100% (four to six animals per group) (C). Representative TEM images of left ventricular muscle collected 4 weeks after surgery. Scale bars: 2 μm (D). *$p<0.01$, MI + saline versus sham + saline; #$p<0.01$, MI + NaHS versus sham + NaHS. &$p<0.05$, MI + NaHS versus MI + saline. NaHS, sodium hydrosulfide; MI, myocardial infarction; NS, not significant; H&E, hematoxylin and eosin; w, week.

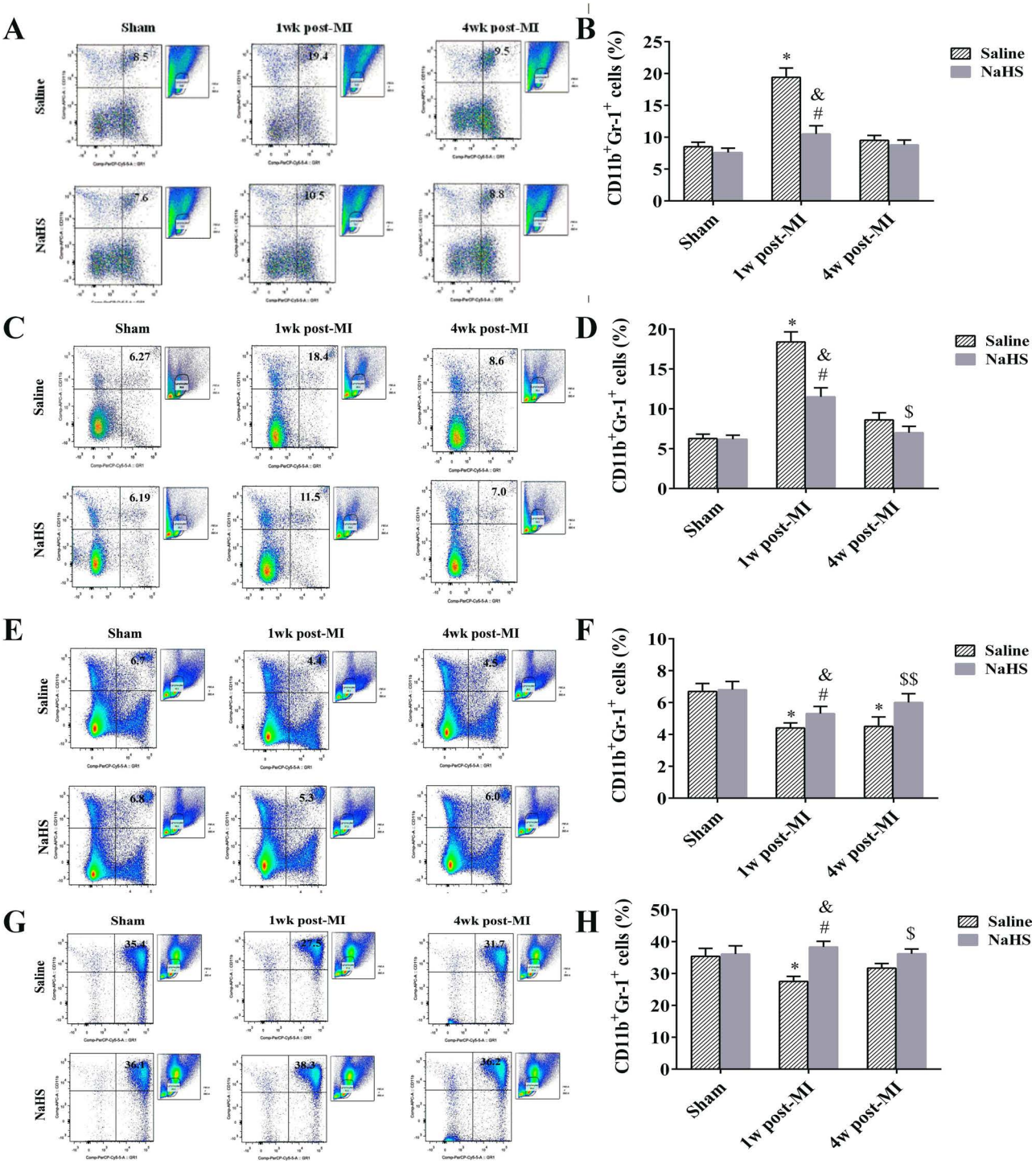

Figure 6. NaHS inhibits recruitment and migration of CD11b$^+$Gr-1$^+$ myeloid cells. Representative flow cytometry dot plots of CD11b$^+$Gr-1$^+$ myeloid cells in myocardium (A), blood (C), spleen (E), and bone marrow (G) 1 week and 4 weeks after surgery. Quantification of CD11b$^+$Gr-1$^+$ cells is also shown for myocardium (B; $n=6$), blood (D; $n=6$), spleen (F; $n=6$), and bone marrow (H; $n=6$). *$p<0.01$, MI + saline versus sham + saline; #$p<0.01$, MI + NaHS versus sham + NaHS. &$p<0.01$, 1 week post-MI + NaHS versus 1 week post-MI + saline. \$$p<0.05$, \$\$$p<0.01$, 4 weeks post-MI + NaHS versus 4 weeks post-MI + saline. NaHS, sodium hydrosulfide; MI, myocardial infarction; NS, not significant; w, week.

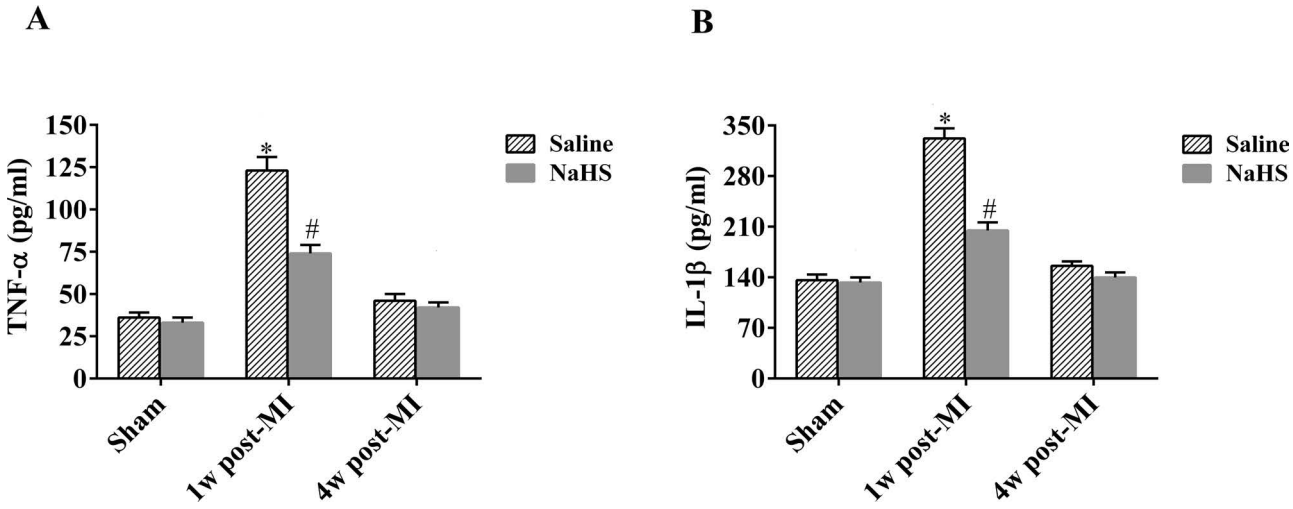

Figure 7. NaHS mitigates inflammatory response in the subacute phase of infarction. Serum TNF-α (A) and IL-1β (B) levels were measured by ELISA 1 week and 4 weeks after occlusion for MI + saline and MI + NaHS groups and 1 week after sham surgery for sham groups ($n = 6$). *$p < 0.01$, MI + saline versus sham + saline; #$p < 0.01$, MI + NaHS versus sham + NaHS. NaHS, sodium hydrosulfide; MI, myocardial infarction; NS, not significant; TNF, tumor necrosis factor; IL, interleukin; w, week.

We found that NaHS-treated mice had a higher rate of survival after coronary occlusion, as well as improved post-MI cardiac function, as determined by M-mode echocardiography, less LV dilatation, and decreased pulmonary edema. These findings suggest that H_2S might be an effective treatment strategy for heart failure induced by chronic myocardial ischemia.

$CD11b^+Gr\text{-}1^+$ myeloid cells are an intrinsic part of the myeloid cell lineage. They are a heterogeneous population composed of myeloid cell progenitors and precursors[25]. The wealth of information that has accumulated in recent years regarding these cells suggests that they might have evolved as a regulatory component of the immune system and probably function as important "gatekeepers" that prevent pathological immune-mediated damage. Although initial observations and most of the current information regarding the role of $CD11b^+Gr\text{-}1^+$ myeloid cells in immune responses have come from studies in the cancer field, accumulating evidence has shown that $CD11b^+Gr\text{-}1^+$ myeloid cells also regulate immune responses in bacterial and parasitic infections, acute and chronic inflammation, traumatic stress, surgical sepsis, and transplantation[26]. In patients, increased levels of blood monocytes during MI correlate with enhanced LV dilation and adverse outcome[27,28]. To our knowledge, the present study is the first to demonstrate that H_2S can substantially reduce mobilization of $CD11b^+Gr\text{-}1^+$ cells from the spleen and lower their numbers in blood and myocardium after MI. These findings could also suggest that decreasing $CD11b^+Gr\text{-}1^+$ cell numbers may preserve cardiac function in the remodeling heart, although we cannot exclude the possibility that H_2S might target other cell types in the healing infarct as well. Thus, H_2S, with its anti-inflammatory properties, should be investigated as a potential treatment to improve infarct healing.

In this study, mouse hearts subjected to coronary occlusion showed dramatic LV remodeling accompanied by dilation and wall thinning at both subacute (1 week after occlusion) and chronic (4 weeks after occlusion) phases of MI. Increased collagen content was found at the site of MI at week 1 and became more advanced thereafter, with collagen continually accumulating over time and totally replacing necrotic myocytes by week 4. This collagen deposition did not occur in mice treated with NaHS immediately before and 1 h after occlusion. Furthermore, collagen content in the scar of MI mice was increased. H_2S has been shown to reduce inflammatory cells and protease activity, which likely changes the balance of matrix breakdown and synthesis[29]. In the present study, we observed increased scar thickness, as measured by Masson staining, indicating that improved healing reduced infarct expansion, which then resulted in attenuated LV remodeling and higher ejection fraction in NaHS-treated mice. H_2S had also been shown to modulate inflammatory cytokines, including NF-κB, IL-6, IL-8, TNF-α, and TGF-β[30–32], to attenuate the inflammatory response in MI, which may also influence LV remodeling and heart failure.

Apoptosis has been shown to be one of the major pathological events involved in the development of cardiac hypertrophy and heart failure induced by myocardial ischemia. A growing body of evidence suggests that apoptosis in cardiomyocytes contributes to the progression of heart failure and that chronic cardiac remodeling

with chamber dilation and impaired systolic function is associated with increased myocyte apoptosis in the infarct border zone after MI[33]. In the current study, a significant increase in apoptotic cardiomyocytes was observed under ischemic condition; nevertheless, the extent of apoptosis was significantly lower in the hearts from NaHS-treated mice compared with the saline controls at 1 and 4 weeks after MI.

In conclusion, we have shown that NaHS treatment can regulate inflammatory response, recruitment of $CD11b^+$ $Gr\text{-}1^+$ cells to myocardium, cardiomyocyte apoptosis, interstitial fibrosis, cardiac hypertrophy and pulmonary edema, LV systolic and diastolic function, and survival after MI. Our findings regarding $CD11b^+Gr\text{-}1^+$ cells suggest that exogenous NaHS has an impact on the innate immune response after MI, which likely contributes to the anti-inflammatory and antiapoptosis effects. Furthermore, this study supports the emerging concept that H_2S treatment might have therapeutic benefits in the setting of ischemia-induced heart failure.

ACKNOWLEDGMENTS: This work was supported by the National Nature Science Foundation of China (No. 81500237) and the China Postdoctoral Science Foundation (No. 2015T8 0464). The authors declare no conflicts of interest.

REFERENCES

1. Krum H, Teerlink JR. Medical therapy for chronic heart failure. Lancet 2011;378:713–21.
2. Frangogiannis NG. Regulation of the inflammatory response in cardiac repair. Circ Res. 2012;110:159–73.
3. Nahrendorf M, Swirski FK, Aikawa E, Stangenberg L, Wurdinger T, Figueiredo JL, Libby P, Weissleder R, Pittet MJ. The healing myocardium sequentially mobilizes two monocyte subsets with divergent and complementary functions. J Exp Med. 2007;204:3037–47.
4. Abe K, Kimura H. The possible role of hydrogen sulfide as an endogenous neuromodulator. J Neurosci. 1996;16:1066–71.
5. Martelli A, Testai L, Breschi MC, Blandizzi C, Virdis A, Taddei S, Calderone V. Hydrogen sulphide: Novel opportunity for drug discovery. Med Res Rev. 2012;32:1093–130.
6. Xiaohui L, Junbao D, Lin S, Jian L, Xiuying T, Jianquang Q, Bing W, Hongfang J, Chaoshu T. Down-regulation of endogenous hydrogen sulfide pathway in pulmonary hypertension and pulmonary vascular structural remodeling induced by high pulmonary blood flow in rats. Circ J. 2005;69:1418–24.
7. Aminzadeh MA, Vaziri ND. Downregulation of the renal and hepatic hydrogen sulfide (H2S)-producing enzymes and capacity in chronic kidney disease. Nephrol Dial Transplant. 2012;27:498–504.
8. Talaei F, Bouma HR, Hylkema MN, Strijkstra AM, Boerema AS, Schmidt M, Henning RH. The role of endogenous H2S formation in reversible remodeling of lung tissue during hibernation in the Syrian hamster. J Exp Biol. 2012;215:2912–9.
9. Cheng Y, Ndisang JF, Tang G, Cao K, Wang R. Hydrogen sulfide-induced relaxation of resistance mesenteric artery beds of rats. Am J Physiol Heart Circ Physiol. 2004;287: H2316–23.
10. Sivarajah A, Collino M, Yasin M, Benetti E, Gallicchio M, Mazzon E, Cuzzocrea S, Fantozzi R, Thiemermann C. Anti-apoptotic and anti-inflammatory effects of hydrogen sulfide in a rat model of regional myocardial I/R. Shock 2009;31:267–74.
11. Olson KR. Hydrogen sulfide and oxygen sensing: Implications in cardiorespiratory control. J Exp Biol. 2008;211: 2727–34.
12. Wallace JL, Vong L, McKnight W, Dicay M, Martin GR. Endogenous and exogenous hydrogen sulfide promotes resolution of colitis in rats. Gastroenterology 2009;137: 569–78, 578.e1.
13. Tamizhselvi R, Koh YH, Sun J, Zhang H, Bhatia M. Hydrogen sulfide induces icam-1 expression and neutrophil adhesion to caerulein-treated pancreatic acinar cells through nf-kappab and src-family kinases pathway. Exp Cell Res. 2010;316:1625–36.
14. Zhang Y, Li H, Zhao G, Sun A, Zong NC, Li Z, Zhu H, Zou Y, Yang X, Ge J. Hydrogen sulfide attenuates the recruitment of CD11b(+)GR-1(+) myeloid cells and regulates Bax/Bcl-2 signaling in myocardial ischemia injury. Sci Rep. 2014;4:4774.
15. Zhang Y, Wang J, Li H, Yuan L, Wang L, Wu B, Ge J. Hydrogen sulfide suppresses transforming growth factor-beta1-induced differentiation of human cardiac fibroblasts into myofibroblasts. Sci China Life Sci. 2015;58:1126–34.
16. Yang XD, Ai W, Asfaha S, Bhagat G, Friedman RA, Jin G, Park H, Shykind B, Diacovo TG, Falus A, Wang TC. Histamine deficiency promotes inflammation-associated carcinogenesis through reduced myeloid maturation and accumulation of CD11b+Ly6G+ immature myeloid cells. Nat Med. 2011;17:87–95.
17. Dobaczewski M, Xia Y, Bujak M, Gonzalez-Quesada C, Frangogiannis NG. CCR5 signaling suppresses inflammation and reduces adverse remodeling of the infarcted heart, mediating recruitment of regulatory T cells. Am J Pathol. 2010;176:2177–87.
18. Huebener P, Abou-Khamis T, Zymek P, Bujak M, Ying X, Chatila K, Haudek S, Thakker G, Frangogiannis NG. CD44 is critically involved in infarct healing by regulating the inflammatory and fibrotic response. J Immunol. 2008;180:2625–33.
19. Shappell SB, Taylor AA, Hughes H, Mitchell JR, Anderson DC, Smith CW. Comparison of antioxidant and nonantioxidant lipoxygenase inhibitors on neutrophil function. Implications for pathogenesis of myocardial reperfusion injury. J Pharmacol Exp Ther. 1990;252:531–8.
20. Shernan SK, Collard CD. Role of the complement system in ischaemic heart disease: Potential for pharmacological intervention. BioDrugs 2001;15:595–607.
21. Venkatachalam K, Prabhu SD, Reddy VS, Boylston WH, Valente AJ, Chandrasekar B. Neutralization of interleukin-18 ameliorates ischemia/reperfusion-induced myocardial injury. J Biol Chem. 2009;284:7853–65.
22. Kondo K, Bhushan S, King AL, Prabhu SD, Hamid T, Koenig S, Murohara T, Predmore BL, Gojon G Sr, Gojon G Jr, Wang R, Karusula N, Nicholson CK, Calvert JW, Lefer DJ. H2S protects against pressure overload-induced heart failure via upregulation of endothelial nitric oxide synthase. Circulation 2013;127:1116–27.
23. Calvert JW, Elston M, Nicholson CK, Gundewar S, Jha S, Elrod JW, Ramachandran A, Lefer DJ. Genetic and pharmacologic hydrogen sulfide therapy attenuates ischemia-induced heart failure in mice. Circulation 2010;122:11–9.

24. Sodha NR, Clements RT, Feng J, Liu Y, Bianchi C, Horvath EM, Szabo C, Sellke FW. The effects of therapeutic sulfide on myocardial apoptosis in response to ischemia-reperfusion injury. Eur J Cardiothorac Surg. 2008;33: 906–13.
25. Kusmartsev S, Nefedova Y, Yoder D, Gabrilovich DI. Antigen-specific inhibition of CD8+ T cell response by immature myeloid cells in cancer is mediated by reactive oxygen species. J Immunol. 2004;172:989–99.
26. Gabrilovich DI, Nagaraj S. Myeloid-derived suppressor cells as regulators of the immune system. Nat Rev Immunol. 2009;9:162–74.
27. Tsujioka H, Imanishi T, Ikejima H, Kuroi A, Takarada S, Tanimoto T, Kitabata H, Okochi K, Arita Y, Ishibashi K, Komukai K, Kataiwa H, Nakamura N, Hirata K, Tanaka A, Akasaka T. Impact of heterogeneity of human peripheral blood monocyte subsets on myocardial salvage in patients with primary acute myocardial infarction. J Am Coll Cardiol. 2009;54:130–8.
28. Mariani M, Fetiveau R, Rossetti E, Poli A, Poletti F, Vandoni P, D'Urbano M, Cafiero F, Mariani G, Klersy C, De Servi S. Significance of total and differential leucocyte count in patients with acute myocardial infarction treated with primary coronary angioplasty. Eur Heart J. 2006;27:2511–5.
29. Mishra PK, Tyagi N, Sen U, Giwimani S, Tyagi SC. H2S ameliorates oxidative and proteolytic stresses and protects the heart against adverse remodeling in chronic heart failure. Am J Physiol Heart Circ Physiol. 2010;298:H451–6.
30. Oh GS, Pae HO, Lee BS, Kim BN, Kim JM, Kim HR, Jeon SB, Jeon WK, Chae HJ, Chung HT. Hydrogen sulfide inhibits nitric oxide production and nuclear factor-kappab via heme oxygenase-1 expression in RAW264.7 macrophages stimulated with lipopolysaccharide. Free Radic Biol Med. 2006;41:106–19.
31. Sodha NR, Clements RT, Feng J, Liu Y, Bianchi C, Horvath EM, Szabo C, Stahl GL, Sellke FW. Hydrogen sulfide therapy attenuates the inflammatory response in a porcine model of myocardial ischemia/reperfusion injury. J Thorac Cardiovasc Surg. 2009;138:977–84.
32. Zhang Z, Chen L, Zhong J, Gao P, Oudit GY. ACE2/Ang-(1–7) signaling and vascular remodeling. Sci China Life Sci. 2014;57:802–8.
33. Whelan RS, Kaplinskiy V, Kitsis RN. Cell death in the pathogenesis of heart disease: Mechanisms and significance. Annu Rev Physiol. 2010;72:19–44.